Long-term acclimation and metabolic responses of eelgrass (*Zostera marina*) clones to a summer heat wave

Master thesis
in the single-subject master program, subject Biological Oceanography
of the Faculty of Mathematics and Natural Sciences
of the Christian-Albrechts-University of Kiel

Submitted by Jana Willim

First examiner:
Prof. Dr. Thorsten B. H. Reusch

Second examiner:
PD Dr. habil. Florian Weinberger

Kiel, May 2023

GEOMAR
Helmholtz Centre for Ocean Research Kiel

Table of Contents

List of Figures

1 Abstract

Ongoing ocean warming driven by climate change is increasing stress on many coastal ecosystems, including seagrass meadows. Like other seagrass species, *Zostera marina* has been shown to be vulnerable to rising sea temperatures, resulting in growth reduction, reduced photosynthesis as well as die-offs of shoots during periods of summer heat waves. For northern temperate populations, a critical threshold temperature has been identified at approximately 25°C. The underlying physiological processes are largely unresolved. While assessments of photosynthesis, growth, and survival provide useful information about plant performance, metabolomics offers a complementary approach to understanding the physiological states of plants under abiotic stress.

Here, I used a long-term heat wave experiment with *Zostera marina* kept in large indoor wave tanks (Zosteratron) over 3 consecutive years. Half of the treatments received three summer heat waves of 26°C, while a second treatment group was only challenged once in the third year. The experiment included three wild-collected clones and was fully crossed. I examined both the primary response of the metabolome of three different clones to an acute heat wave, as well as potential acclimation from the two preceding years.

I found a small but detectable impact of the heat treatment on the metabolome three weeks after the heat wave. However, no evidence of an acclimation process was observed. The metabolome of *Zostera marina* leaves was found to be mainly affected by clone affiliation. Notably, one clone exhibited significantly higher quantities of targeted metabolites and the most robust growth rates compared to the red and yellow clones.

Metabolomics provided a detailed insight into the phenotypic response of *Zostera marina* leaves to heat wave treatment and clone affiliation. The results suggest responses to environmental stressors in terms of their metabolomic reactions may be very clone-specific in *Zostera marina*. This finding emphasizes the importance of genotype selection in the restoration process. Assisted evolution strategies are already discussed in order to enhance the thermal resilience of coral reefs and could also be implemented in seagrass meadow restoration in the future.

2   Introduction

Seagrasses are a group of flowering plants that grow in shallow marine and estuarine environments around the world. They are essential to structure and function of marine ecosystems. Seagrass meadows provide important ecosystem services, such as maintaining water quality, stabilizing sediments, storage of carbon dioxide emissions and providing habitat for a wide variety of marine organisms (see Figure 1) (Duarte et al., 2013, Fourqurean et al., 2012; Gattuso et al., 2018; Röhr et al., 2016; Unsworth et al., 2015). The seagrass meadows in the western Baltic Sea consist of the common seagrass *Zostera marina* L., a species with very high ecological tolerance and global distribution (Yu et al., 2022), but without any redundancy at species level in this region.

Like other seagrass species, *Zostera marina* is vulnerable to various stressors, including rising sea temperatures. In fact, die-offs of shoots are regularly observed during short periods of exceptionally warm water that can last days to weeks (Hammer et al., 2018; Plaisted et al., 2022; Reusch et al., 2005). This vulnerability is exacerbated by ongoing climate change, which is causing the Baltic Sea to warm at three times the rate of the global ocean. Moreover, the likelihood of summer heat waves is expected to increase even more, further adding on the problem (Meier et al., 2022). According to the IPCC 2021 report, heat waves that currently occur once every hundred years are expected to happen every ten years by the end of the century. The Baltic Sea ecosystem may suffer greatly as a result of these prolonged heat waves (Frölicher & Laufkötter, 2018; Meier et al., 2022; Oliver et al., n.d.). Heat stress may lead to a drastic decline in seagrass beds in the future. At water temperatures of 25°C and above, a stress response of plants is measurable in the form of lower or stopped growth rates, reduced photosynthetic rate and increased shoot mortality (Bergmann et al., 2010; Franssen et al., 2014; Jueterbock et al., 2016; Moreno-Mar In et al., 2018; Nejrup & Pedersen, 2008; Reusch et al., 2005, Reusch et al., unpublished). The underlying physiological processes are largely unresolved. High temperatures can damage the photosynthetic apparatus within the plant, leading to a decline in photosynthetic rates (e.g. Collier et al., 2012); the efficiency of processes like nutrient uptake and assimilation, which are essential for plant growth, can be reduced (e.g. Pazzaglia et al., 2020) and the plant's immune system can be weakened, making it more vulnerable to infection by pathogens (e.g. Olsen & Duarte, 2015)

A complementary approach to understanding the physiological states of plants under abiotic stress is metabolomics, which offers information about the physiological states of plants under abiotic stress in addition to assessments of photosynthesis, growth, and survival. (Lawson et al., 2022). The exponential increase in the number of articles utilizing metabolomics

to study plants under abiotic stress over the last decade underscores its efficacy (Anzano et al., 2021).

With the frequency and severity of heat waves projected to increase with climate change (Meier et al., 2022), investigating the acclimation potential and metabolic responses of seagrasses to heat stress is crucial for their survival. While adaptation is a population's long-term, irreversible response to a change in its environment that happens over several generations through natural selection, acclimation is an organism's short-term, reversible response to a particular environmental stressor (Borowitzka, 2018). Importantly, adaptation is a process at the population level and ultimately involves changes in gene or allele frequencies (Bock, 1980), while acclimation is a process on the individual genotype level. Acclimation can involve changes in a variety of physiological processes, including metabolism, respiration, photosynthesis, and water balance (e.g. Lagerspetz, 2006). The thermal priming effect is a type of acclimation that occurs in response to a short-term exposure to a moderate stressor, such as a brief period of elevated temperature. This exposure can induce genetic modifications and changes in an organism's physiology that enhance its ability to tolerate subsequent, more severe stressors of the same type, such as longer exposure to high temperatures (e.g. Hossain et al., 2018).

The existence of a thermal priming effect, whereby prior exposure to a sub-lethal heat stress event can increase the plants' tolerance to subsequent heat stress events, has been documented in a number of studies on seagrasses. For example, Nguyen et al., 2020 found that *Zostera muelleri* plants, that experienced two consecutive heat waves days to weeks before a targeted heat stress exposure, showed improved resistance measured by photosynthetic activity and growth. Similarly, Pazzaglia et al. (2022) reported a thermal priming effect of *Posidonia oceanica* seedlings. The exact mechanisms behind the thermal priming effect are not yet fully understood, but may involve modification at molecular and epigenetic levels, metabolism, and cellular signalling pathways (Gu et al., 2012). Understanding these mechanisms is critical for developing effective strategies to mitigate the impacts of heat stress on seagrass ecosystem, which is hence a focus of this thesis.

Among with acclimation to heat stress (heat hardening), other assisted evolution strategies are also discussed in order to enhance the thermal resilience of seagrass meadows in the future (Pazzaglia et al., 2021a). Assisted evolution, also known as human-assisted evolution or facilitated adaptation, refers to the deliberate and intentional actions taken by humans to accelerate the evolutionary processes of a species in response to environmental pressures or changes (Van Oppen et al., 2015). For example, a targeted selection of heat tolerant genotypes as founder plants for seagrass meadow restoration would be a measure of the assisted evolution toolbox.

Identifying metabolites that indicate heat stress and heat coping capacity could enable this selection of heat-tolerant plants. A few studies have already found evidence for heat stress in the metabolome. Hammer et al. (2018) could identify metabolic regulations of seagrass under heat stress. Metabolites connected to the nitrogen cycle (amino acids, urea, GABA) were downregulated, whereas soluble sugars were found in higher quantities. Other studies found the carbohydrate metabolism especially affected by heat stress in terrestrial plants (Guy et al., 2008). Additionally, many proteins were found degraded (Franssen et al., 2011), whereas heat shock proteins were produced (Marín-Guirao et al., 2016). Ideally, the identified metabolites can be utilized as biomarkers for stress levels, circumventing the need to conduct lengthy and costly experiments (Kuzhiumparambil et al., 2022).

As the importance of active restoration of ecosystems gains recognition at the national and international political level, also marine ecosystem restoration has become a priority. In order to prevent ecosystem degradation and support restoration efforts, the UN established the Decade for Ecosystem Restoration in 2022. Meanwhile, the EU has announced a law for the restoration of nature's ecosystems, which includes marine habitats (Halleux, 2022). These developments highlight the need for a better understanding of the physiological mechanisms that enable plant species like *Zostera marina* to thrive in challenging environments, and metabolomics is proving to be a valuable tool for this purpose.

Seagrass forms the basis for the local ecosystem and creates a productive habitat for diverse species. Fish, starfish, crustaceans and other sea dwellers find food between the leaves of the grass and use it as a refugium from predators (Larkum et al., 2006). For fish, such as the Baltic herring (*Clupea harengus*, L.), seagrass beds function as spawning grounds and nurseries (von Nordheim et al., 2018). In this way, they contribute to securing fish stocks in the Baltic Sea.
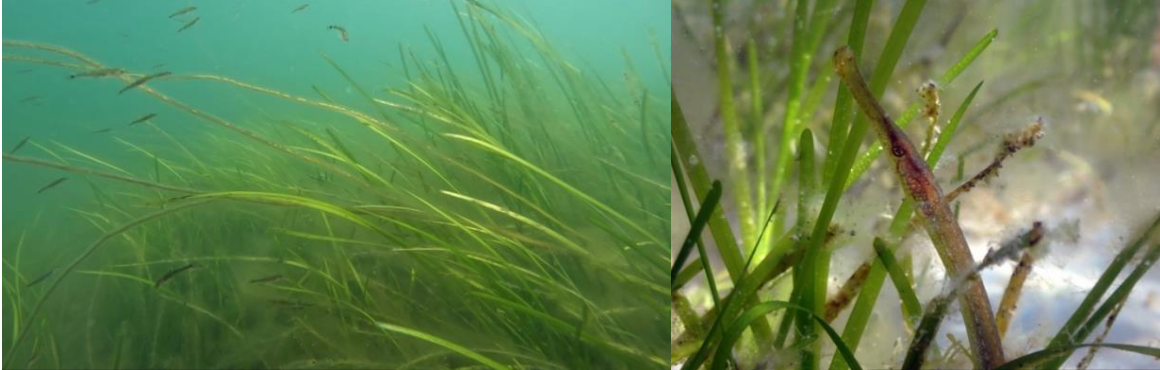
Seagrass slows down the current velocity and prevents erosion (Fonseca et al., 1983; Patriquin, 1975). Thus, seagrass is actively involved in coastal protection (Duarte et al., 2013).

The number of potential harmful bacteria is reduced by a seagrass community (Reusch et al., 2021).

Seagrass meadows function as a blue carbon sink (Fourqurean et al., 2012). Carbon dioxide is stored long-term in the sediment via rhizomes and root systems. According to estimates, the carbon pool of a seagrass meadow in the Baltic Sea is between 6.98 and 44.9 t C ha-1 (Röhr et al., 2016). In other words, it stores one ton CO_2 per hectare per year. Therefore, seagrass is proposed as a nature-based solution to mitigate human carbon emissions (Gattuso et al., 2018). Other results have focused on eelgrass loss as a source for Carbon and Nitrogen in the ocean, which estimated values of 60.2 Mg C and 6.63 Mg N per hectare and economic cost to society of 7944 and 141,355 US$/ha (Moksnes et al., 2021).

Figure 1: Seagrass and its diverse functions and ecosystem services; Upper left photo by Jana Willim: intact seagrass meadow, upper right photo by Philipp Süßle: pipefish hiding between seagrass leaves, middle left photo by Philipp Süßle: houses behind a seagrass meadow, middle photo: illustration of the habitus of Zostera marina by Jana Willim; middle right photo by CDC: vibrio bacteria, lower left photo by Angela Stevenson: Jana Willim taking sediment cores in a seagrass meadow

3   Hypotheses

This study tested the effects of an acute heat wave (heat wave 21) on the metabolome composition and the quantities of these metabolites depending on:

1) previous heat stress experience
2) genotype (= clone) affiliation
3) and the combination of both

I hypothesized that the effects of experimental heat waves can be found in characteristic patterns of the metabolome of a seagrass leaf.

The heat wave effects were tested on different sets of response variables:

- the general metabolome composition and the quantities of these metabolites
- targeted metabolites, which can be taken as biomarkers indicating heat stress
- moreover, leaf growth rates were assessed as one key phenotypic performance variable

The analytical strategy of the metabolomic analysis consisted of two steps. First, signals of the multi-variate non-targeted metabolome composition were analysed. In a second step, metabolites with a high explanatory value for their group (see 1 to 3) are in focus. These targeted metabolites were identified by Random Forest algorithm and analysed via ANOVA. This study focuses on the heat wave recovery phase, three weeks after the heat wave.

4   Material and Methods

General experimental outline

Heat stress effects on Zostera marina were examined by simulating heat waves in indoor wave tanks over three years (the "Zosteratron"), with half of the treatments receiving two heat waves in the preceding year 2019 and 2020, before the assessment year in 2021 ("acute heat wave"), while the other half of replicates were exposed to high summer temperatures only in 2021. Via mass spectrometric measurements, the metabolites contained in leaf tissue were analysed. Along with the general metabolome composition and targeted metabolites, leaf growth measurements were conducted and evaluated. In this manner, the scope of long-term acclimation to heat waves, as well as individual differences among genotypes are evaluated.

Study Design

The aim of the experiment was to simulate a summer heat wave scenario in indoor mesocosms. This was achieved through a gradual increase in temperature until the absolute water temperature reached ~26°C and was maintained for three weeks. This treatment level caused heat stress in *Zostera marina* from the area in previous studies (e. g. Bergmann et al., 2010b; Franssen et al., 2014b). Control tanks, on the other hand, were always kept at temperatures that are optimal for Baltic eelgrass (≤21°C). Natural sand filtered seawater was supplied to tanks measuring 160 cm (length) x 45 cm (width) x 80 cm (height) from the Kiel fjord, and lamps with a diel cycle are used to replicate daylight, providing around 150 micromole quanta m^{-2} s^{-1} at the leaf surface. Additionally, an artificial wave with a frequency of approx. 0.5 Hz ensured typical orbital water movements for coastal areas, thus the natural conditions.

The study design considered two critical factors that may impact individual plant performance during and after the experiment. Firstly, the genetic background of the plants was taken into account, with three wild-collected different clones used in the experiment, which allowed the comparison of genetically different individuals. Secondly, the heat treatment history of the last three years is also considered, and the samples for metabolomic analysis were taken after the third year of treatment. Each clone and treatment history in combination with the acute heat wave has three replicates available.

Figure 2 illustrates all treatment combinations. After sampling at Falckenstein beach, Kiel the shoots of each of the three clones were divided into two groups. One group experienced a heat wave in the summer of 2019 and in the summer of 2020 and the other group stayed at a physiologically normal temperature for the whole time. In the summer of 2021, the groups were subdivided into a group that was exposed to a heat wave in this year

and one that did not get one. As a result, four different types of treatment history occur: some individuals experienced a heat wave in each of the three summers, some individuals experienced two summers of heat waves and in the last summer not, others never experienced a heat wave and another group of individuals has not had a heat wave in the first and second summer and then in 2021 they were exposed to their very first heat wave.

This design allowed the investigating the effect of an acute heat wave, as well as the testing of acclimatization by comparing individuals that already experienced two previous heat waves before and individuals that suffer for the first time from a heat wave. In addition to the metabolomics approach, the various collaborators of this large-scale experiments have collected data on leaf histology, leaf growth, shoot production, and photosynthetic activity (via PAM), while a transcriptome analysis via RNAseq is planned.

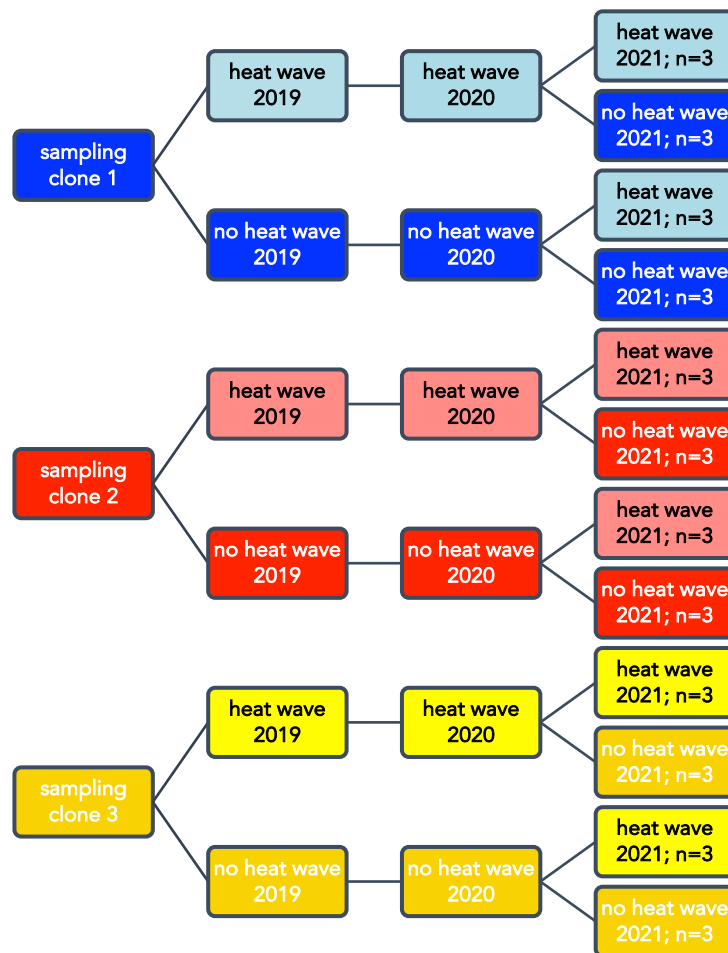*Figure 2: Experimental Design for multi-year heat wave acclimation experiment in Zostera marina*

Heat waves are indicated in pale colour; no heat waves are indicated in intense colour; a heat wave is defined as a water temperature rise about 6°C above the usual temperature (~19°C to ~25°C) for four weeks, excluding a stepwise heating and cooling period. Three samples of each subgroup were taken for metabolomic analyses.

Tissue Sampling

Tissue sampling for the metabolomic assessment was performed on 24 September 2021 during the recovery phase three weeks after the heat wave from 12 August to 2 September 2021. The recovery phase was chosen for investigation to assess the persistent long term stress status rather than the acute stress. The youngest leaf of the plant was carefully excised from the leaf sheath and a 2.5 cm long part tissue segment, protected from epiphytic contamination, was employed as the sampling material. The specimens were promptly deposited in 2.5 mL Eppendorf vials and flash-frozen in liquid nitrogen. Preservation of the samples was ensured by storage at - 80°C until extraction. In total 36 samples were used for metabolomic analyses, divided in three replicates per subgroup (3 clones * 4 heat treatment histories; Figure 2).

Leaf Growth Rates

Growth rates were determined at the beginning, in the middle, at the end of the heat wave and in the recovery phase. Shoots were marked with cable ties at the base and the length of the three youngest leaves were measured with a ruler at intervals of four days relative to the transparent leaf sheet. The growth of all growing leaves (typically leaf 1 and 2) was added up and divided by the days. Care was taken to detect and measure any newly formed leaves during the measurement interval.

Metabolome Extraction and Mass-Spectrometry

Metabolome extraction followed a modified protocol by Matyash et al. (2008) and utilized the polar phase for analysis. The Fourier-transform ion cyclotron resonance mass spectrometry (FT-ICR-MS) instrument (7 Tesla, SolariXR, Bruker, Bremen, Germany) was used with water/methanol (1:1) as the transport eluent and an electrospray ionization method was applied. The instrument has a detection range of 65 to 1200 Da, an average resolution of 600,000 at 400 m/z, a time-of-flight time section of 0.35-1.2 ms, and a quadrupole mass of 150 m/z with an RF frequency of 2 MHz. Data output was assessed using the MetaboScape 2021b software from Bruker (Bremen, Germany) and further annotated with the SmartFormular feature via a previously created annotation list. Additionally, identification was done via investigation of sum formulas using search engines like lotus, PubChem and ChemSpider. Sum formulas and identified metabolites might deviate as they could not be determined with a 100% accuracy. The identification level of the identified metabolites is based on Sumner et al. (2007) a level four identification.

Data Analysis and Statistics

All statistical analyses were performed in R 4.2.2. (R Core Team, 2022). Metabolites detected by FT-ICR-M were filtered prior data analysis. Metabolites that were at least in one third of the samples in at least one analytical group abundant and additionally had a fold change of ≤ 1.0 (corresponds to reducing of intensity under stress) or ≥ 1 (corresponds to enhancing of intensity under stress) were filtered for the following statistical analyses. In total 1,019 metabolites passed the filtering. NAs were seen as measurements under the detection limit of 100,000 counts and were replaced by 999,999.

Multivariate and targeted statistical analyses were used for the metabolome dataset. In a first step, a permutational analysis of variance (PERMNOVA, R-package "vegan" Oksanen J et al., 2022) using the Bray-Curtis dissimilarities of the full dataset was performed including all 1,019 metabolites as response distance matrix. The acute heat wave (Heat wave 21; levels = cold, warm) and temperature history (levels = cold, warm) were included, while setting clone (levels = blue, red, yellow) as strata (i.e., random factor) and ran the model with 150,000 permutations. As a previously implemented test for multivariate homogeneity of group dispersions of the distance matrices among all treatment levels yielded no deviation. The predictor effects assessed via PERMANOVA base on differences in group centroids rather than differences in group dispersions (Anderson et al., 2013). The results of PERMANOVA were illustrated with 3D MDS plots (R-package "vegan3d" Oksanen et al., 2023). The grouping factors heat wave 21, Clone affiliation and the combination of heat wave 21 and clone affiliation were selected for further analysis. Heat wave history and the interaction heat of wave history and/or heat wave 21 and/or clone affiliation was just in one case significant, which is shown in Figure 4. For the rest of the analysis heat wave history was omitted as a grouping factor.

As a second step in multivariate metabolome analyses, I applied a classification approach for the pre-determined phenotypes/treatments, which is a critical component in utilizing metabolomics data for examining their explanatory potential. This study used the Random Forest model, which performs better than other methods for identifying key-metabolites for group discrimination (such as PLS-DA) because it is capable of handling unbalanced designs, missing values, and missing covariance among many metabolic features (Trainor et al., 2017). Random Forest models in R (R-package "randomForest", Liaw & Wiener, 2002; R-package "party", Strobl et al., 2008) were fitted to predict the group identity of plant individuals for Heat wave 21 in combination with clone affiliation (blue-cold, blue-warm, read-cold, red-warm, yellow-cold, yellow-warm) based on their metabolome. The results of the analysis were the Random Forest classification trees, which were based on 2,000 individual decision trees and accepted 30 randomly chosen metabolites as candidates for each split. The mean decrease in accuracy (MDA) of the grouping prediction upon removal of the relevant

metabolite from the model was employed to determine the relevance of a metabolite in predicting a given group identity.

The 30 highest-ranking metabolites selected by Random Forest were subsequently analysed using ANOVA. Metabolites, that showed a significant interaction for the interaction of heat wave 21 and clone affiliation were chosen for targeted analysis. The results are shown in bar plots. Metabolites that did not show a significant interaction between heat wave 21 and clone affiliation were not pursued for further study as they were deemed inadequate as biomarker candidates.

The single metabolites chosen for targeted analysis, as well as the variable leaf growth were analysed with generalized linear mixed effects models (G)LMMs with the R-package "glmmTMB" (Brooks Met al., 2017). The Kolmogorov-Smirnov test for uniformity and the nonparametric dispersion test, which are both included in the R-package "DHARMa" (Hartig, 2022). for targeted model optimisation, were used to choose the best fitted model. Based on computed confidence limits, type III ANOVAs were performed to analyse the models that best fit the data for leaf growth rates and each metabolite (Fox & Weisberg, 2019; R-package "car"). Based on Wald-x? tests, type III ANOVA tables were calculated using sum-to-zero contrasts for all factors (R-package "car", Fox & Weisberg, 2019). If heat wave history and/or clone affiliation were significant interaction variables, post-hoc comparisons between the estimated marginal means of their factor levels solely within levels of other interaction factor levels were calculated using R-package "emmeans" (Lenth, 2023). Using the R-package "insight" (Lüdecke et al., 2019) and the R-package "effectsize" (Ben-Shachar et al., 2020), variance components were extracted from all models, and model parameter estimates were standardised for comparative illustration.

5   Results

Effects of heat wave history, acute heat stress and clone affiliation on growth rates

The study examined the effect of an ongoing heat wave on the growth rate of leaves. At the beginning of the heat wave the clones differed among one another (Table 1) in leaf growth rate (Table 1), with ramets of the blue clone growing fastest at about 7 cm (SE ± 0.6) per day (Figure 3; Table 1 Appendix), followed by the yellow (6 cm per day, SE ± 0.6) and red clone (4.5 cm per day, SE ± 0.6). During the acute heat wave the growth rates are significantly lower under elevated temperatures, while the clone affiliation had no significant impact (Table 1). Heat stressed plants grew by 1-2 cm (SE ± 0.2) slower per day less than controls (Figure 3; Table 1 Appendix). After the heat wave the clone affiliation has a significant impact again. Also, the interaction of the heat wave history and the heat wave 2021 is significant. During the recovery phase, growth rates are restored and revealed only little difference among heat treated and control plants (0.5-1 cm per day, SE ± 0.4; P = 0.089, Table 1). Whereas the heat-treated leaves of the blue clone grew about 1 cm (SE ± 0.4) per day faster than the ones of the red clone and about 0.2 cm (SE ± 0.4) per day faster than the yellow clone (Figure 3, Appendix Table 1).

The interaction of heat wave treatment history with any other factor or factor combination had no detectable effects on leaf growth with one exception. After the acute heat wave, plants that had experienced previous heat waves in 2019/2020 showed slower (by about 1cm per day, SE ± 0.3) leaf growth rates than plants with no heat wave history (Table 1; Figure 4). Accordingly, the heat wave treatment history was statistically marginally significant but only during the last sampling date (Table 1, P = 0.079).

Table 1: Two-factorial Analysis of variance: effects of heat history and acute heat wave on leaf growth (.p<0.1, *p<0.05, **p<0.01, ***p<0.001; Significant results are shown in bold), total n=36

	Start heat wave	Mid heat wave	End heat wave	Recovery Phase
Clone 3 levels, 12 replicates per level	**P = 0.006 **** **$F_{(2,33)}$= 6.27**	P = 0.343 $F_{(2,33)}$= 1.12	P = 0.432 $F_{(2,33)}$= 0.87	**P = 0.016 *** **$F_{(2,33)}$= 4.94**
Heat wave 21 2 levels, 18 replicates per level	P = 0.962 $F_{(1,35)}$= 0.00	**P = < 0.001 ***** **$F_{(1,35)}$=18.84**	**P = <0.001 ***** **$F_{(1,35)}$= 71.86**	**P = 0.089** **$F_{(1,35)}$= 3.14**
Heat wave history 2 levels, 18 replicates per level	P = 0.8684 $F_{(1,35)}$= = 0.03	P = 0.297 $F_{(1,35)}$= 1.14	P = 0.250 $F_{(1,35)}$= 1.39	P = 0.419 $F_{(1,35)}$= 0.68
Clone * Heat wave 21 6 levels, 6 replicates per level	P = 0.689 $F_{(5,30)}$= 0.38	P = 0.337 $F_{(5,30)}$= 1.14	P = 0.582 $F_{(5,30)}$= 0.55	P = 0.460 $F_{(5,30)}$= 0.80
Clone * Heat wave history 6 levels, 6 replicates per level	P = 0.983 $F_{(5,30)}$= 0.02	P = 0.359 $F_{(5,30)}$= 1.07	P = 0.873 $F_{(5,30)}$= 0.14	P = 0.968 $F_{(5,30)}$= 0.03
Heat wave 21 * Heat wave history 4 levels, 8 replicates per level	P = 0.549 $F_{(3,32)}$= 0.37	P = 0.923 $F_{(3,32)}$= 0.01	P = 0.652 $F_{(3,32)}$= 0.21	**P = 0.079 .** **$F_{(3,32)}$= 3.36**

Growth rates
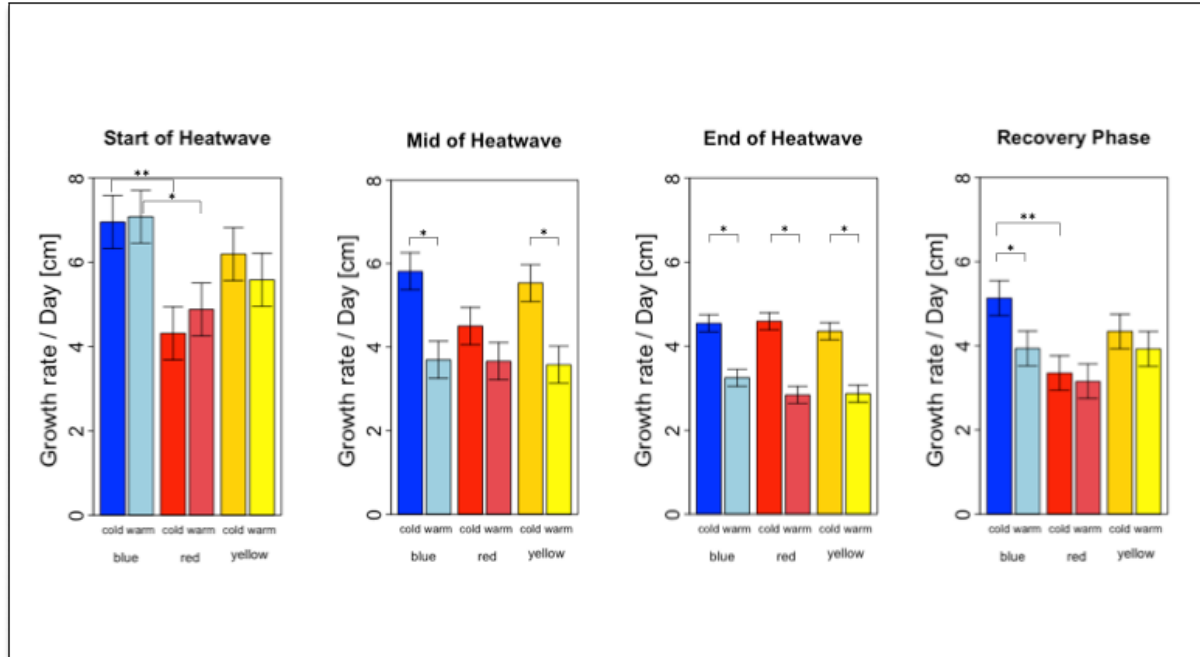
Figure 3: Leaf growth rates of eelgrass (Zostera marina) during for time points during the heat wave 2021; Growth rates at the beginning, the middle, the end of the heat wave and during the recovery phase, bar plots show means of for leaf growth rates (n=9 per timepoint) with standard errors predicted by (G)GLMNs. Elongation of all growing leaves was added up. Measurements of three plants growing in the same box were averaged. Horizontal lines with asterisks within plots indicate post-hoc comparisons (.p<0.07, *p<0.05, **p<0.01, ***p<0.001).
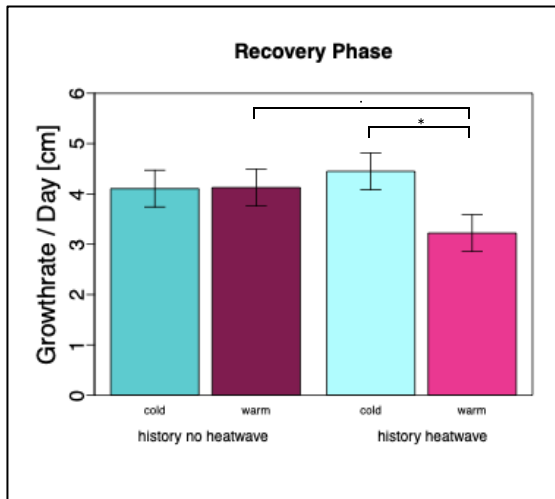
Figure 4: Leaf growth rate per day during the recovery phase; Bar plots show means of for leaf growth rates (n=9) with standard errors predicted by (G)GLMNs. Horizontal lines with asterisks within plots indicate post-hoc comparisons (.p<0.07, *p<0.05, **p<0.01, ***p<0.001). The two left columns show leaf growth rates for shoots that have not discovered a heat wave in 2019 and 2020, the two right columns show leaf growth rates for shoots that have discovered a heat wave in 2019 and 2020; blue colour indicates no heat wave in 2021 and pink colour indicates heat wave in 2021; leaves that discovered a heat wave in all three years have the lowest growth rate (about 1 cm per day lower than the controls) and differ significantly (P = 0.079, $F_{(3,32)}$ = 3.36, Df = 1).

Multivariate statistical analyses

Table 2: PERMANOVA analysis on a dataset of 1019 metabolites extracted from Zostera marina, subjected to a summer heat wave. The clone affiliation has a strong significant impact on the leaf metabolome. The acute heat wave treatment in 2021 effects the metabolome slightly significant. The heat wave history and the interaction between clone and heat wave 2021 was not significant. (number of permutation: 150000,; .p<0.07, *p<0.05, **p<0.01, ***p<0.001; Significant results are shown in bold).

Clone	Acute heat wave	Heat wave History	Clone * Acute heat wave	Clone * Heat wave history	Acute heat wave * Heat wave history
P=<0.001 ***	**P = 0.0536 .**	P = 0.515	P = 0.371	P = 0.919	P = 0.315
F(2,33)= 4.75	**F(1,35)= 1.72**	F(1,35)= 0.91	F(30,5)= 1.05	F(30,5)= 0.68	F(3,32)= 1.10
Df = 2	**Df = 1**	Df = 1	Df = 2	Df =2	Df = 1

The entire dataset (1,019 metabolites) was analysed using PERMANOVA (Table 2). I found significant differences in the composition of leaf metabolites among clone affiliation and the acute heat wave treatment in 2021. Although the combination of heat wave 2021 and clone was not significant, further exploratory analysis of the interaction was nevertheless done as the single parameters were significant. The impact of the heat wave history on the metabolome was not significant in any factor combination and was hence neglected subsequently from further analysis to preserve the statistical power of the remaining treatment factors by enhancing denominator degrees of freedom.

Under the acute heat wave treatment small significant differences in the composition of leaf metabolites were found compared to controls (Figure 5 and Table 2). The corresponding NMDS plot showed two distinct treatment groups that partially overlap (Figure 5). A Random Forest algorithm predicted the treatment group in 54% of runs correctly. The prediction for the control group (cold) was in 64% of runs predicted correctly, whereas the heat wave treated group was in 45% of replicate runs predicted correctly.

Figure 5: NMDS plot and Random Forest algorithm depicting the main effects of heat wave 2021 on leaf metabolite composition. Significant main effects of the simulated heat wave in 2021 on the composition of 1019 leaf metabolites in Zostera marina assed via PERMANOVA and Random Forest models. The PERMANOVA results are illustrated along with NMDS plots with spider bodies (groupwise centroids) and ellipses (groupwise standard error). Turquoise color indicates the control group and deep pink color indicates heat wave treatment group. Stacked bar plots represent the confusion matrix of supervised Random Forest models predicting the temperature treatment of plants from their leaf metabolome. They quantify the fraction of plants that was predictively assigned to a given category. Percentage values for the fraction of correct predictions in each observed category are denoted within the correspondingly colored block with the models' overall out of bag error (oob) estimated at the top.

The composition of leaf metabolites differed significantly among replicated ramets of the three clones (Figure 6). The NMDS plot revealed three differentiated centroids, with the blue clone more separated from both, the red and the yellow clone. Random Forest models were the most accurate when predicting clone affiliation compared to the acute heat wave groups or the combination of both (out of bag error: clone affiliation < heat wave 21 < combination of both; see Random Forest Predictions Figure 5, 6 and 7), with the red clone having 100% accuracy, while the blue and yellow clones had 83% accuracy, as shown in Figure 6. In total predictions of clone affiliation were in 87% of the tries wrong (oob=13%).
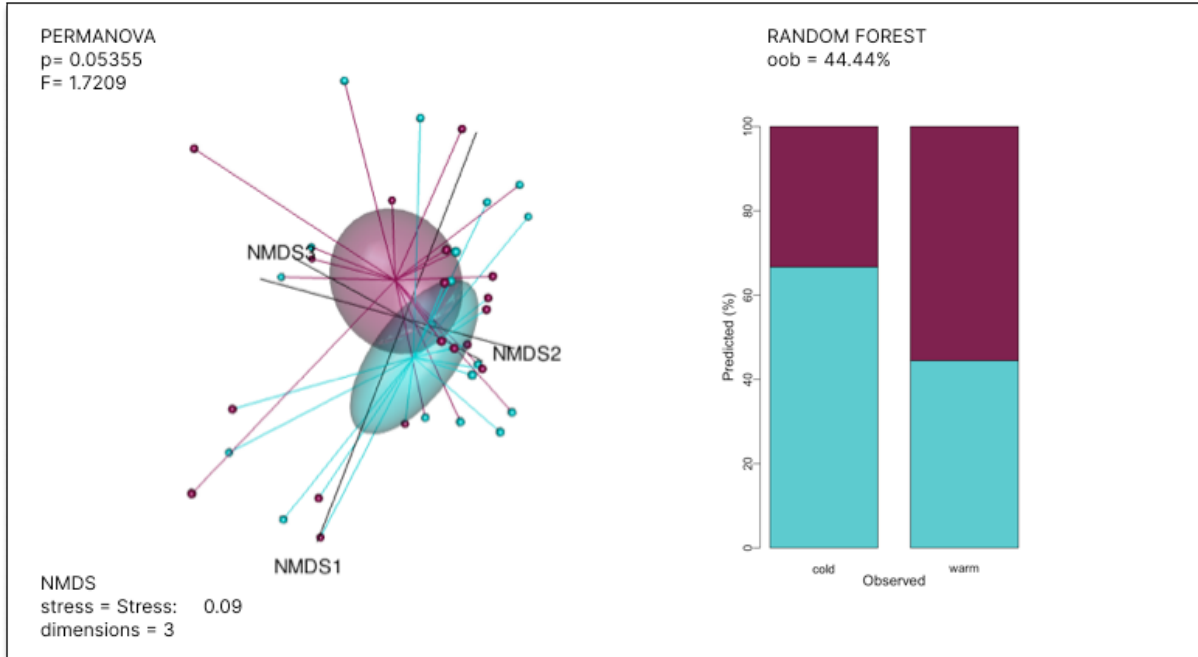
Figure 6: NMDS plot and Random Forest algorithm depicting the main effects of clone affiliation on leaf metabolite composition. Significant main effects of the simulated heat wave in 2021 on the composition of 1019 leaf metabolites in Zostera marina assessed via PERMANOVA and Random Forest models. The PERMANOVA results are illustrated along with NMDS plots with spider bodies (groupwise centroids) and ellipses (groupwise standard error). Colors indicate clone affiliation (blue, red, yellow). Stacked bar plots represent the confusion matrix of supervised Random Forest models predicting the clone affiliation of plants from their leaf metabolome. They quantify the fraction of plants that was predictively assigned to a given category. Percentage values for the fraction of correct predictions in each observed category are denoted within the correspondingly colored block with the models' overall out of bag error (oob) estimated at the top.

However, when factors "acute heat wave" and "clone" were combined, there were no significant differences in metabolite composition revealed by PERMANOVA (Table 2), although there was a trend of group differentiations apparent in the NMDS plot (Figure 7). The centroids are separating samples belonging to the same clone, while another separation driven by acute heat treatment is also visible. The predictions by Random Forest of the acute heat wave treatments in combination with the clone affiliation had an out of back error of approximately 63%, as shown in Figure 7. When neglecting incorrect predictions of the heat treatment, the correct clone affiliation could be predicted by Random Forest to at least 75%.
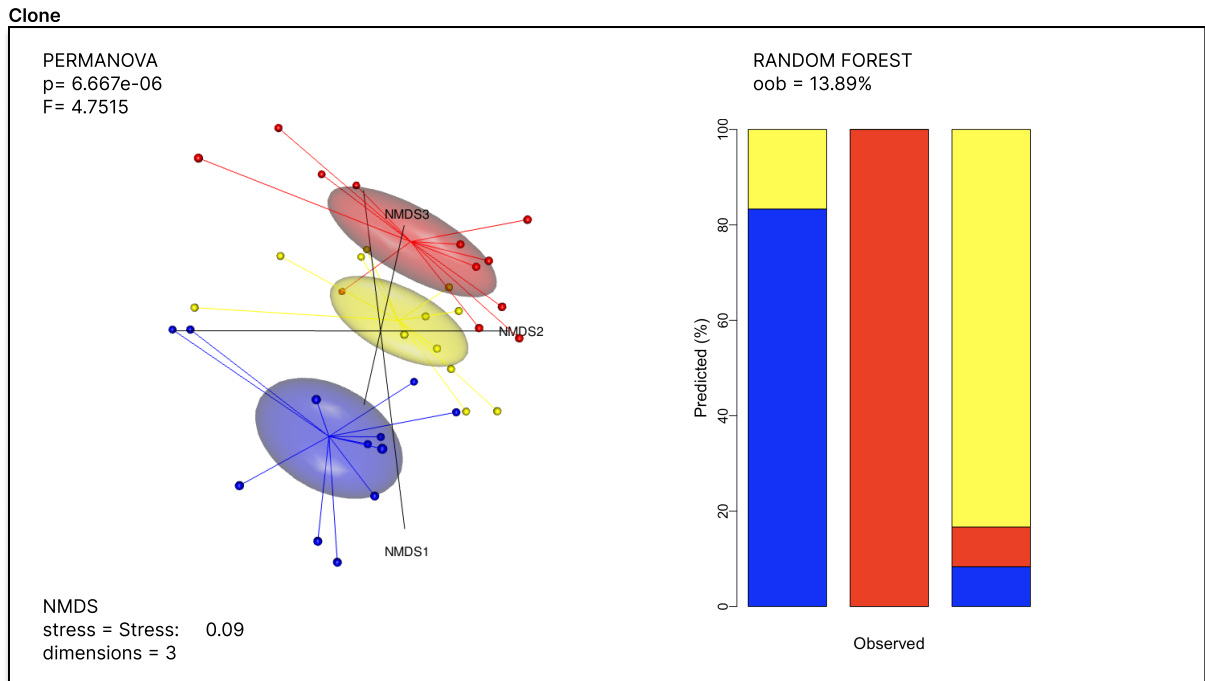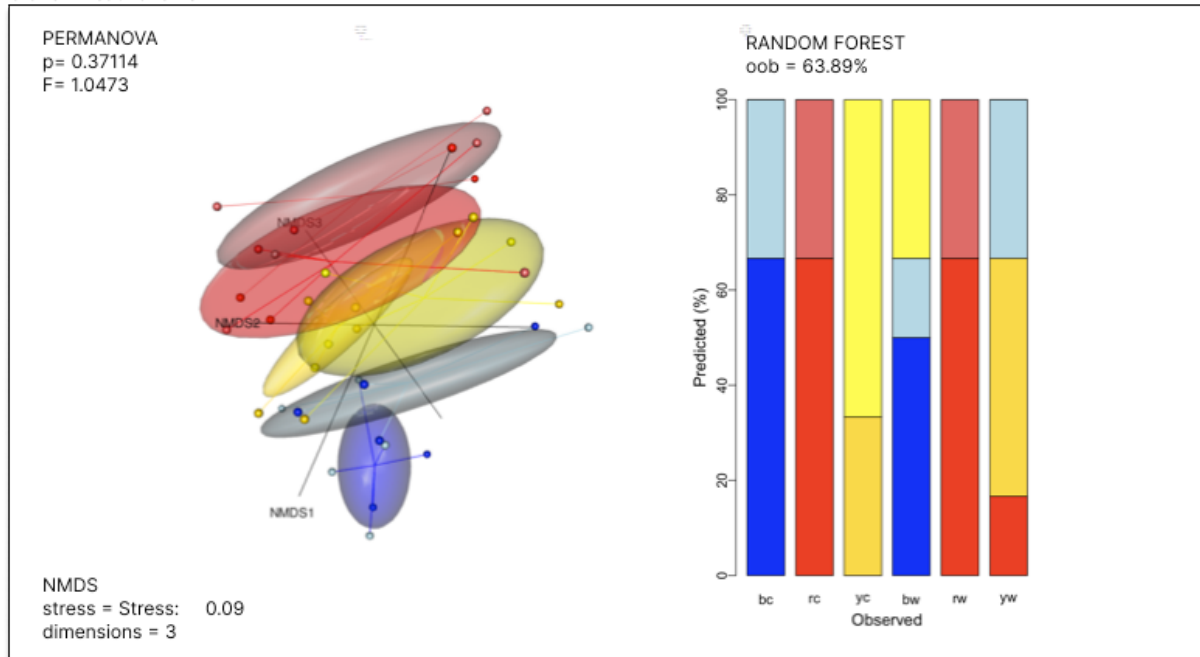
Figure 7: NMDS plot and Random Forest algorithm depicting the main effects of Heat wave 2021 and clone affiliation on leaf metabolite composition. Significant main effects of the simulated heat wave in 2021 on the composition of 1019 leaf metabolites in Zostera marina assed via PERMANOVA and Random Forest models. The PERMANOVA results are illustrated along with NMDS plots with spider bodies (groupwise centroids) and ellipses (groupwise standard error). Colors indicate clone affiliation (blue, red, yellow), light color stands for heat wave treatment. Stacked bar plots represent the confusion matrix of supervised Random Forest models predicting the temperature treatment in combination with the clone affiliation of plants from their leaf metabolome. They quantify the fraction of plants that was predictively assigned to a given category. Percentage values for the fraction of correct predictions in each observed category are denoted within the correspondingly colored block with the models' overall out of bag error (oob) estimated at the top.

Targeted statistical analyses

The top 30 metabolites for group separation picked by Random Forest caused a mean decrease accuracy of group prediction ranging from seven to four percent (Figure 8 left side). To address differences in metabolic responses among clone affiliation and heat treatment histories, ANOVAs analyzing the interaction were performed (Figure 8 right side). While the clone affiliation had a significant effect for all 30 tested metabolites, this applied for only 8 metabolites with respect to factor "acute heat wave". The interaction "acute heat wave * clone affiliation" was significant in 15 cases, which were then further analysed by performing (G)LMMs. Results are shown in bar plots in Figure 9. To simplify the readability of the plots, metabolites are coded (M01 to M30) in Figures 8 + 9 and in the following text.

The metabolomes of the three clones were found to be different, including the regulation of the metabolites under acute heat stress (Figure 9). The intensity of one metabolite decreased in one clone, whereas the intensity for another clone increased. In general, the metabolome of the blue clone is more different to the metabolome of the red and the yellow clone. Most of the investigated metabolites were found in highest quantities in the blue clone

(Figure 9). Exceptions were $C_6H_{17}NO_3S_2$ (M13) and $C_{10}H_{12}O_6$ (M29), which were the most abundant in the red clone. $C_7H_3N_3O_5S$ (M28) had the highest quantity in the yellow clone. The metabolite $C_6H_8O_4$ (M06) is likely ethyl maleate. The molecule $C_{10}H_{12}O_6$ (M29) was found to be a monoterpenoid. Terpenoids are the largest and most diverse group of secondary metabolites in plants, but metabolic pathways and composition are highly modified in the model seagrass *Zostera marina* (Olsen et al., 2016). They are known to play important roles in plant defence against biotic and abiotic stresses, such as heat stress (Singh & Sharma, 2015). The intensities of $C_{10}H_{12}O_6$ (M29) change clone-specific in opposite directions after the plants experienced heat stress. The intensities of the not treated plants of the blue and the red clone are very similar. After the acute heat wave the intensity of $C_{10}H_{12}O_6$ (M29) decreased by about 60% in the blue clone while it increased by about 30% in the red clone. $C_{13}H_{10}O_5$ (M18) is most likely a phenylpropanoid. It has been suggested that the metabolite may be a type of furocoumarin, which is recognized for its ability to regulate heat shock genes (Al Kordy, 1998). $C_6H_{12}O_6$ (M20) and $C_5H_{13}O_7P$ (M23) are monosaccharides. The other metabolites could not be identified.

Metabolite	H 21	Clone	H21 * Clone
M01		***	
M02		***	*
M03		***	*
M04		***	
M05		***	
M06		***	.
M07		***	
M08	.	***	
M09	.	***	
M10		***	
M11		***	
M12		.	
M13	*	***	.
M14	.	***	***
M15		***	
M16		***	***
M17		***	
M18		***	**
M19		***	*
M20	.	**	**
M21	**	***	**
M22		***	
M23		***	*
M24		***	
M25		***	*
M26	*	***	
M27	*	*	***
M28		***	*
M29		***	*
M30		***	
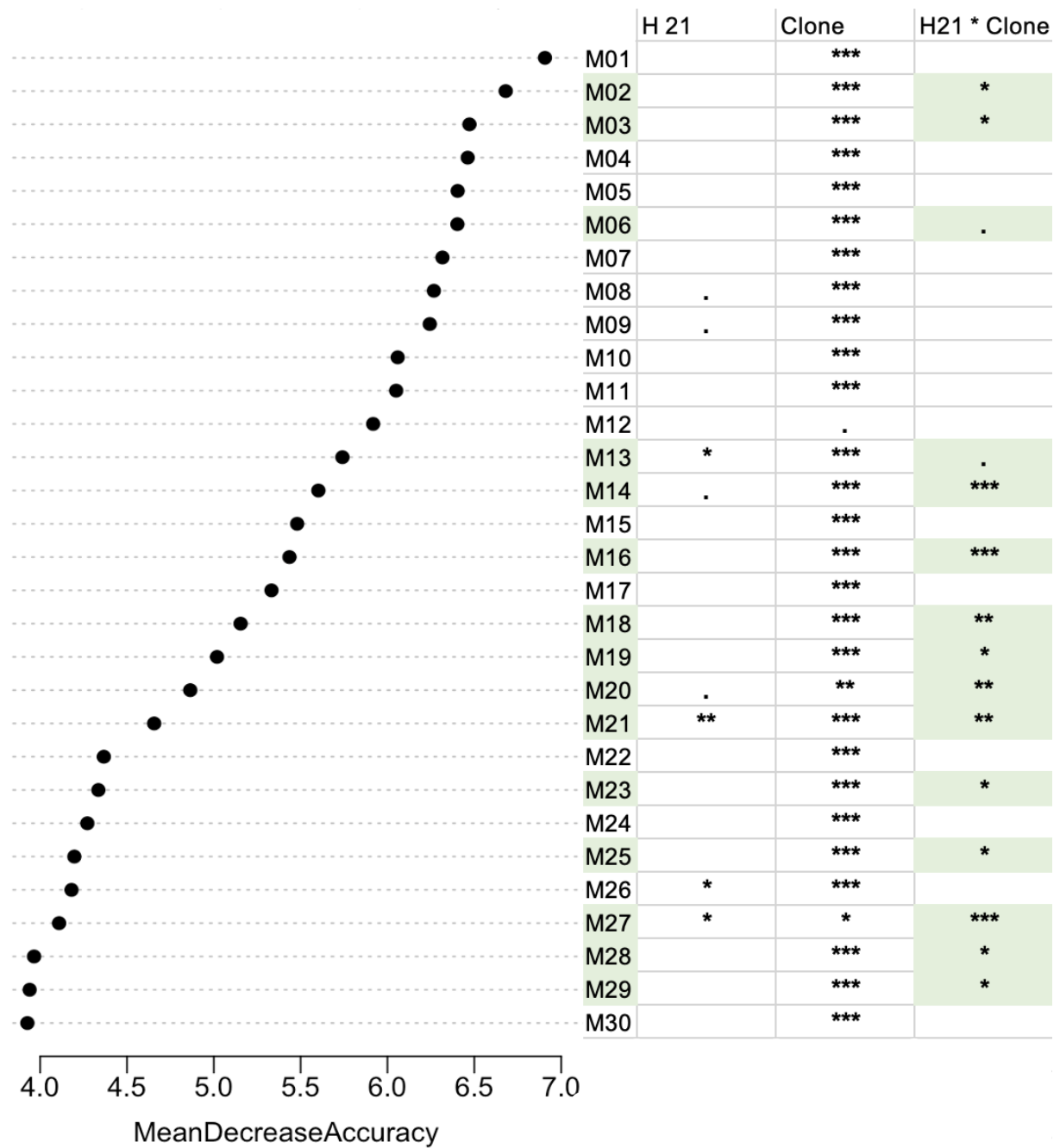
*Figure 8: Top 30 metabolites identified by Random Forest. The removal of from the model of the single metabolites caused a high mean decrease in prediction accuracy. Table displays significance levels of acute heat wave (H 21), the clone affiliation (Clone) and the interaction of the acute heat wave and clone affiliation interaction (H 21*Clone) via 2-way ANOVA (.<0.1,*p<0.05, **p<0.01, ***p<0.001). Metabolites that showed a significant interaction of acute heat wave * clone affiliation are marked in green and are displayed as bar plots in Figure 9.*
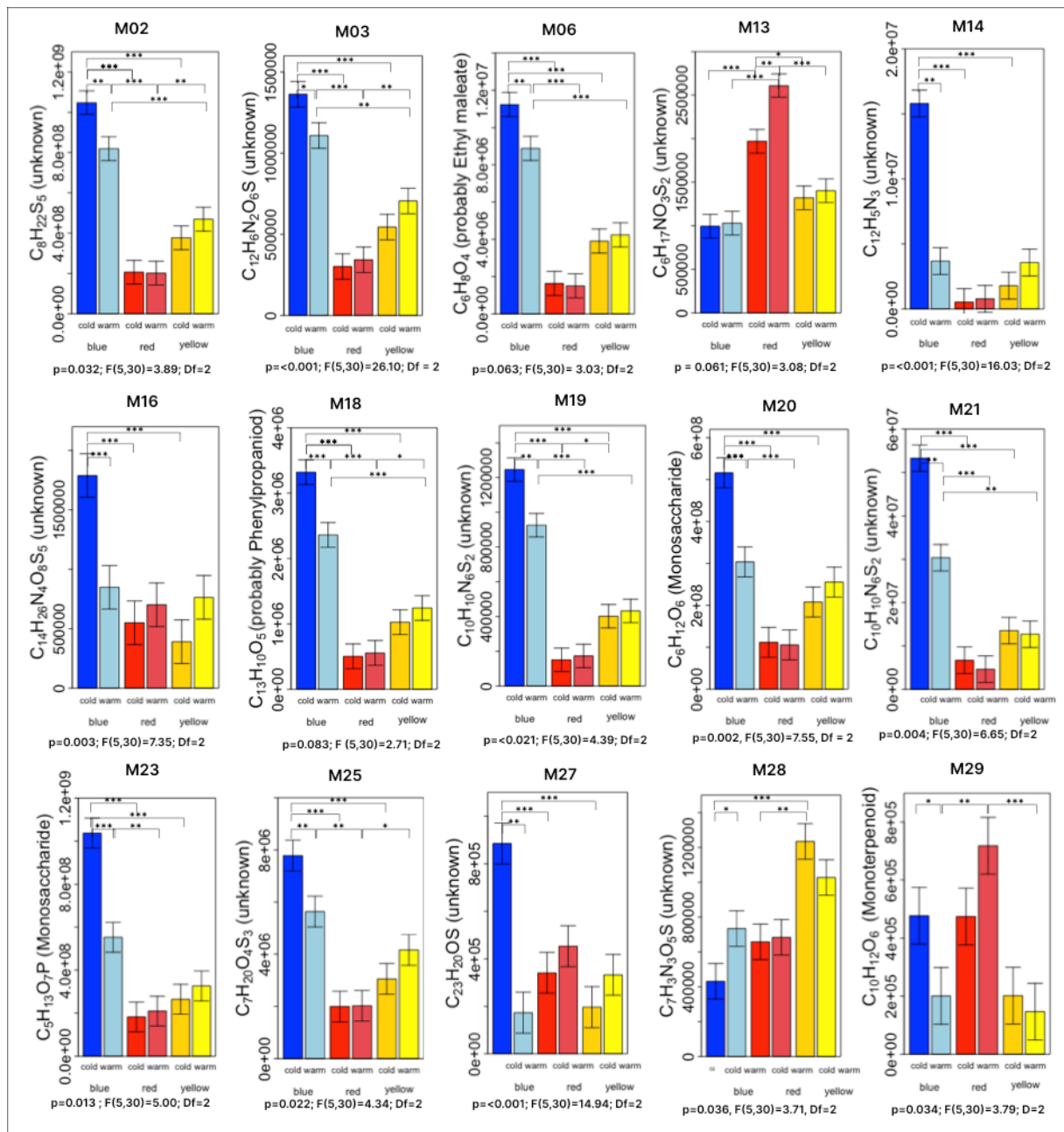
Figure 9: Targeted metabolome analyses of the acute heat wave in combination to clone affiliation for metabolites identified through Random Forest and tested for significant effects of acute heat wave * clone affiliation interaction via 2-way ANOVA. Bar plots show means of for metabolite intensities with standard errors predicted by (G)GLMNs. Horizontal lines with asterisks within plots indicate post-hoc comparisons (*p<0.05, **p<0.01, ***p<0.001). Below each panel, the ANOVA results of the interaction are given.

6   Discussion

This study revealed that the metabolome of *Zostera marina* leaves was influenced by clone affiliation along with the impact of an acute heat wave, simulating the expected increase of summer heat waves. Qualitatively, the effects of clone affiliation were more pronounced as for the acute heat wave, while both were interacting when focusing on targeted metabolites selected based on Random Forest algorithms. Given that I analysed the metabolome three weeks after the return to normal temperatures, the persistent effect on the metabolome was surprising and indicated longer lasting effects and delayed recovery, while negative effects on leaf growth had nearly vanished. Notably, one clone exhibited deviated in its pattern of untargeted and in targeted metabolites. Furthermore, the blue clone had the most robust growth rates compared to the red and yellow clones.

Analysis of the growth rates and the metabolome revealed no evidence of a long-term acclimation process (Table 1 and 2) in response to heat treatment history. The hypothesis that plants that experienced heat waves in previous years acclimate long-term to heat and exhibit superior performance following a final challenge ("acute heat wave") compared to naive plants was not confirmed. Moreover, in one instance, pooled over clones, plants showed a delayed recovery when they had experienced three consecutive heat waves, rather than a single one (Figure 4), suggesting rather an accumulation of adverse effects over the years, than long-term acclimation. This effect was only marginally significant ($F_{(3,32)}$=3.36, P=0.079; Table 1) and requires further study.

Other studies found a priming effect when repeatedly exposing seagrasses (*Zostera muelleri; Posidonia australis*) to heatwaves with short (days to weeks) recovery intervals in between (Nguyen et al., 2020). In Baltic *Zostera marina* a phenotypic plasticity in response to temperature on the morphology level was recently discovered. When leaves were exposed to a heat wave, their aerenchyma - the tissue responsible for exchanging respiratory gases - undergoes enlargement of about 56% in mean aerenchymae surface cross section (P=<0.001, $F_{(1,23)}$=14.60, Df=1; Wirries, 2023). Due to improved gas exchange, this enlargement probably benefits raising respiration rates when under heat stress. On a time scale of a few weeks, which corresponds to the length of earlier experiments, the enlarged aerenchyma are likely persistent but reversible on an inter-annual time scale. This discrepancy may explain why Nguyen et al. (2020) discovered a priming effect, whereas this study on an inter-annual time scale found no evidence of long-term acclimation. The finding of aerenchyma enlargement might be an example for many more ongoing plastic changes induced by heat stress and their reversibility.

In response to an acute heat wave, leaf growth rates decreased during and after the temperature exposure, demonstrating that the chosen experimental temperature conditions of approximately three weeks at 26°C indeed constituted a stress for the plants. Leaf growth rates of *Zostera marina* differed between ramets of the three different clones during the recovery phase. The difference in growth rates between the heat wave treated group and the control group were marginal, indicating rapid recovery of heat stressed *Zostera marina* plants within the four weeks after the end of the thermal stress. In parallel the metabolome response was small but detectable. In contrast, during the heat wave, leaf growth rates were significantly reduced by 13 to 15% (range over clones) under thermal stress (Table 1), in accordance with previous studies in Zostera marina from northern Europe (Hammer et al., 2018).

Despite this, the impact of the acute heat waves on seagrass *Zostera marina* not only affected leaf growth rates but also resulted in changes in the metabolome composition measured during the recovery phase. Metabolomics gave a detailed insight into the physiological processes of the three different genotypes (Figure 6) and the effect of an acute heat wave (Figure 5), which both had a significant effect on the metabolome (Table 1). When the factor of the acute heat wave (heat wave 21) in interaction with clone affiliation were tested on the whole metabolome set, the PERMANOVA did not reveal a significant interaction, but a trend of group differentiation was observed, as shown in the NMDS plot in Figure 7. Random Forest models were in most cases able to predict the clone affiliation but made mistakes predicting the heat treatment (Figure 7) indicating that the clone-specific metabolome pattern is more specific than the impact of an acute heatwave.

When I moved on to test those metabolites with the highest explanatory value for treatment group and clone affiliation (targeted analysis), several substances revealed a significant interaction between clone affiliation and acute heat wave exposure, revealing interesting clone specific reaction to acute heat wave, that potentially have functions as biomarkers. By examining those metabolites, a more complex understanding of the phenotypic response can be obtained.

In detail, the acute heat wave in 2021 did not result a clear up- or downregulation of intensities of the investigated metabolites (Figure 9). Rather, heat stress has increased the plasticity of the individual metabolites. This became apparent when looking at the interactive effect of acute heat wave and clone affiliation (Figure 9). Here, the targeted metabolites of the leaves in controls of the blue clone appear again in highest intensities compared to the other clones, except for $C_6H_{17}NO_3S_2$ (M13), $C_{10}H_{12}O_6$ (M29) und $C_7H_3N_3O_5S$ (M28), which were found in the red and yellow clone in higher intensities. Furthermore, the heat wave has resulted in a notable decrease in intensity of the specific metabolites in the blue clone, whereas these metabolites in other clones decreased. Nevertheless, intensities of the blue clone remained in highest intensities in most cases (Figure 9). The non-targeted analysis of the whole

metabolome, shown in the NMDS plot in Figure 6, revealed the same trend: the blue clone was more distant in the three-dimensional matrix to the red and the yellow clone. These observations lead to the assumption that the metabolite composition is primarily governed by two key determinants, namely the main effect of clone affiliation and the clone-specific reactions to heat stress. These factors were identified as the most significant contributors to the observed metabolic variations and collectively influence the specific up- or downregulation of metabolites, which are probably connected to certain metabolic pathways. The before described pathway regulations involving the nitrogen cycle (Hammer et al., 2018), protein degradation (Guy et al., 2008) or heat shock protein synthesis (Marín-Guirao et al., 2016) could not be observed to be the main drivers of the metabolome characteristics in this study. The metabolites for targeted analysis of this study were not picked by pathway interaction, as a high identification level of metabolites according to Sumner et al. (2007) could not be achieved using FT-ICR-MS without fragmentation mode. Instead, a fingerprint of the phenotypic metabolic status after experiencing an acute heat wave was revealed. Hereby, it could be shown that it is possible to find group separating metabolites, that could potentially be applied as biomarkers for variation in specific traits.

Zostera marina plants display significant variation in shoot production, biomass and nutrient uptake rates, as well as in stress responses and recovery processes among individual clones, as evidenced by previous findings by Hughes et al. (2009) and Salo et al. (2015). Accordingly, this study reveals a remarkable amount of variation among just three randomly selected clones from a single site, located only 15 meters apart (Figure 9). Scaling the clone-specific responses to environmental stressors influencing the metabolism of Zostera marina to a larger scale, these findings strongly suggest that there exists significant genetic and phenotypic diversity in the south-western Baltic Sea. One example of this study is the blue clone. Ramets of this clone revealed in all tested metabolites a higher quantity than the red and the yellow clone. In addition, the leaves of the blue clone contained significantly more monosaccharides.

In conclusion, the substantial changes in the metabolome composition revealed significant metabolic plasticity during the heat wave, and it is likely that specific metabolites are causal in identifying the clones that are more resilient to the effects of rising heat waves in the Baltic Sea. In line with a recent study (Ventura et al., 2022) I discovered that the metabolic reconfiguration could be implemented to generate empirically testable hypotheses for subsequent in-depth examination of the metabolic mechanisms that mitigate or precipitate heat-induced damages in seagrasses.

As soon as we have a more mechanistic understanding, selected metabolites can be used for developing more effective biomonitoring and management strategies for ecosystems, including those relevant for seagrass conservation and management. In detail, metabolites

could be used as biomarkers to test the phenotypic tolerance to heat stress in an effective way. Further, the acquired knowledge from metabolomic analysis can be integrated with other study parameters, such as the fully sequenced reference genome (Van de Peer et al., 2021), transcriptomic data, and morphological and histological changes, to obtain a more comprehensive understanding of the underlying processes triggered by heat stress (Gazeau et al., 2018) in *Zostera marina*.

Outlook

A promising approach of developing future effective restoration strategies for seagrass meadows is the identification of genotypic and phenotypic variations in the metabolomic profiles, along with their corresponding levels of tolerance to heat wave events. Currently, the ongoing efforts on Assisted Evolution approaches are just starting to be implemented for seagrass species, such as *Posidonia oceanica* (Pazzaglia, 2022; Pazzaglia, Nguyen, et al., 2021b; Pazzaglia, Reusch, et al., 2021). In that respect, the seagrass ecology and evolution field is about ten years behind the coral ecology community. However, with the accelerating effects of climate change, there is an urgent need to improve the survival prediction and sustainability of restoration projects for native seagrass. For example, the current method of randomly selecting shoots from a donor meadow as founder plants in restoration projects could be improved, as it is unclear whether the selected genotypes will withstand future water temperatures. To make renaturation more sustainable, selecting heat tolerant genotypes as founder plants is crucial. Therefore, this study emphasizes the importance of genotype selection in the restoration process.

In conclusion, a metabolomic testing protocol via biomarkers can be developed to evaluate the heat tolerance of seagrass genotypes, making it simple to select certain genotypes for restoration projects. One next objective to put my current data into context would be to investigate the impact of an acute heat wave on the metabolome, not just during the recovery phase. The identification of more specific metabolites associated indicating acute heat stress would be a central step towards developing a comprehensive metabolomic testing protocol for seagrass restoration.

7 Acknowledgements

Firstly, I would like to express my gratitude to Prof. Dr. Thorsten Reusch for giving me the chance to conduct a research topic that I am passionate about, and for his support throughout the process. His advice and mentoring have played a major role in forming my knowledge of the topic and in developing my research skills. I would also like to thank Anna Bockelmann and Diana Gill for their assistance with sampling. In the lab of Prof. Dr. Karin Schwarz's research group at Kiel University, the extraction and Mass-Spectrometry analysis were conducted. Dr. Tobias Demetrowitsch made an essential contribution to this collaboration. In order to complete the analytics, Dr. Karin Schrieber from Kiel University lent her statistical expertise to the project, which I am very thankful for. Further, I would like to express my gratitude to Dr. Florian Weinberger for agreeing on the role as the second examiner. Finally, I extend my appreciation to my friends for their companionship throughout the course of this thesis.

Literature

Al Kordy, M. A. (1998). Selection for yield and chromones quality in khella [ammi visnaga l]. III. allelopathic expressions and chemotypes X environmental interaction. *Bulletin of Faculty of Pharmacy-Cairo University*, *36*(3), 157–170.

Anderson, Marti J, Walsh, Daniel C, & e.al. (2013). PERMANOVA, ANOSIM, and the Mantel test in the face of heterogeneous dispersions: What null hypothesis are you testing? *Ecological Monographs*, *83*(4), 557–574. https://doi.org/https://doi.org/10.1890/12-2010.1

Anzano, A., Bonanomi, G., Mazzoleni, S., & Lanzotti, V. (2021). Plant metabolomics in biotic and abiotic stress: a critical overview. In *Phytochemistry Reviews*. Springer Science and Business Media B.V. https://doi.org/10.1007/s11101-021-09786-w

Ben-Shachar M, Lüdecke D, & Makowski D. (2020). effectsize: Estimation of Effect Size Indices and Standardized Parameters. *Journal of Open Source Software*, *5*(56).

Bergmann, N., Winters, G., Rauch, G., Eizaguirre, C., Gu, J., Nelle, P., Fricke, B., & Reusch, T. B. H. (2010a). Population-specificity of heat stress gene induction in northern and southern eelgrass Zostera marina populations under simulated global warming. *Molecular Ecology*, *19*(14), 2870–2883. https://doi.org/10.1111/j.1365-294X.2010.04731.x

Bergmann, N., Winters, G., Rauch, G., Eizaguirre, C., Gu, J., Nelle, P., Fricke, B., & Reusch, T. B. H. (2010b). Population-specificity of heat stress gene induction in northern and southern eelgrass Zostera marina populations under simulated global warming. *Molecular Ecology*, *19*(14), 2870–2883. https://doi.org/https://doi.org/10.1111/j.1365-294X.2010.04731.x

Bock, W. J. (1980). The Definition and Recognition of Biological Adaptation1. *American Zoologist*, *20*(1), 217–227. https://doi.org/10.1093/icb/20.1.217

Borowitzka, M. A. (2018). The 'stress' concept in microalgal biology—homeostasis, acclimation and adaptation. *Journal of Applied Phycology*, *30*(5), 2815–2825. https://doi.org/10.1007/s10811-018-1399-0

Brooks, Kristensen K, van Benthem K, Magnusson A, Berg C, Nielsen A, Skaug H, Maechler M, & Bolker B. (2017). glmmTMB Balances Speed and Flexibility Among Packages for Zero-inflated Generalized Linear Mixed Modeling. *The R Journal*, *9*(2), 378–400.

Collier, C., Uthicke, S., & Waycott, M. (2012). Thermal tolerance of two seagrass species at contrasting light levels: Implications for future distribution in the Great Barrier Reef. *Limnology and Oceanography*, *56*, 2200–2210. https://doi.org/10.4319/lo.2011.56.6.2200

Duarte, C. M., Losada, I. J., Hendriks, I. E., Mazarrasa, I., & Marbà, N. (2013). The role of coastal plant communities for climate change mitigation and adaptation. *Nature Climate Change*, *3*(11), 961–968. https://doi.org/10.1038/nclimate1970

Fonseca, M. S., Zieman, J. C., Thayer, G. W., & Fisher, J. S. (1983). The role of current velocity in structuring eelgrass (Zostera marina L.) meadows. *Estuarine, Coastal and Shelf Science*, *17*(4), 367–380. https://doi.org/https://doi.org/10.1016/0272-7714(83)90123-3

Fourqurean, J. W., Duarte, C. M., Kennedy, H., Marbà, N., Holmer, M., Mateo, M. A., Apostolaki, E. T., Kendrick, G. A., Krause-Jensen, D., McGlathery, K. J., & Serrano, O. (2012). Seagrass ecosystems as a globally significant carbon stock. *Nature Geoscience*, *5*(7), 505–509. https://doi.org/10.1038/ngeo1477

Fox J, & Weisberg S. (2019). *An {R} Companion to Applied Regression, Third Edition. Thousand Oaks CA: Sage.* https://socialsciences.mcmaster.ca/jfox/Books/Companion/

Franssen, S. U., Gu, J., Bergmann, N., Winters, G., Klostermeier, U. C., Rosenstiel, P., Bornberg-Bauer, E., & Reusch, T. B. H. (2011). Transcriptomic resilience to global warming in the seagrass Zostera marina, a marine foundation species. *Proceedings of the National Academy of Sciences of the United States of America*, *108*(48), 19276–19281. https://doi.org/10.1073/pnas.1107680108

Franssen, S. U., Gu, J., Winters, G., Huylmans, A. K., Wienpahl, I., Sparwel, M., Coyer, J. A., Olsen, J. L., Reusch, T. B. H., & Bornberg-Bauer, E. (2014a). Genome-wide transcriptomic responses of the seagrasses Zostera marina and Nanozostera noltii under a simulated heatwave confirm functional types. *Marine Genomics*, *15*, 65–73. https://doi.org/10.1016/j.margen.2014.03.004

Franssen, S. U., Gu, J., Winters, G., Huylmans, A.-K., Wienpahl, I., Sparwel, M., Coyer, J. A., Olsen, J. L., Reusch, T. B. H., & Bornberg-Bauer, E. (2014b). Genome-wide transcriptomic responses of the seagrasses Zostera marina and Nanozostera noltii under a simulated heatwave confirm functional types. *Marine Genomics*, *15*, 65–73. https://doi.org/https://doi.org/10.1016/j.margen.2014.03.004

Frölicher, T. L., & Laufkötter, C. (2018). Emerging risks from marine heat waves. In *Nature Communications* (Vol. 9, Issue 1). Nature Publishing Group. https://doi.org/10.1038/s41467-018-03163-6

Gattuso, J. P., Magnan, A. K., Bopp, L., Cheung, W. W. L., Duarte, C. M., Hinkel, J., Mcleod, E., Micheli, F., Oschlies, A., Williamson, P., Billé, R., Chalastani, V. I., Gates, R. D., Irisson, J. O., Middelburg, J. J., Pörtner, H. O., & Rau, G. H. (2018). Ocean solutions to address climate change and its effects on marine ecosystems. *Frontiers in Marine Science*, *5*(OCT). https://doi.org/10.3389/fmars.2018.00337

Gazeau, F., Tuya, F., Zimmer, M., Duarte, B., Martins, I., Rosa, R., Matos, A. R., Roleda, M. Y., Reusch, T. B. H., Engelen, A. H., Serrão, E. A., Pearson, G. A., Marques, J. C., Caçador, I., Duarte, C. M., & Jueterbock, A. (2018). Climate Change Impacts on Seagrass Meadows and Macroalgal Forests: An Integrative Perspective on Acclimation and Adaptation Potential. *Frontiers in Marine Science | Www.Frontiersin.Org*, *1*, 190. https://doi.org/10.3389/fmars.2018.00190

Gu, J., Weber, K., Klemp, E., Winters, G., Franssen, S. U., Wienpahl, I., Huylmans, A. K., Zecher, K., Reusch, T. B. H., Bornberg-Bauer, E., & Weber, A. P. M. (2012). Identifying core features of adaptive metabolic mechanisms for chronic heat stress attenuation contributing to systems robustness. In *Integrative Biology* (Vol. 4, Issue 5, pp. 480–493). https://doi.org/10.1039/c2ib00109h

Guy, C., Kaplan, F., Kopka, J., Selbig, J., & Hincha, D. K. (2008). Metabolomics of temperature stress. In *Physiologia Plantarum* (Vol. 132, Issue 2, pp. 220–235). https://doi.org/10.1111/j.1399-3054.2007.00999.x

Halleux, V. (2022). *BRIEFING Laufende Legislativverfahren der EU EPRS | Wissenschaftlicher Dienst des Europäischen Parlaments*.

Hammer, K. J., Borum, J., Hasler-Sheetal, H., Shields, E. C., Sand-Jensen, K., & Moore, K. A. (2018). High temperatures cause reduced growth, plant death and metabolic changes in eelgrass Zostera marina. *Marine Ecology Progress Series*, *604*, 121–132. https://doi.org/10.3354/meps12740

Hartig F. (2022). *_DHARMa: Residual Diagnostics for Hierarchical (Multi-Level / Mixed) Regression Models_. R package version 0.4.6*. https://CRAN.R-project.org/package=DHARMa

Hossain, M. A., Li, Z.-G., Hoque, T., Burritt, D., Fujita, M., & Munné-Bosch, S. (2018). Heat or cold priming-induced cross-tolerance to abiotic stresses in plants: key regulators and possible mechanisms. *Protoplasma*, *255*. https://doi.org/10.1007/s00709-017-1150-8

Hughes, A. R., Stachowicz, J. J., & Williams, S. L. (2009). Morphological and physiological variation among seagrass (Zostera marina) genotypes. *Oecologia*, *159*(4), 725–733. https://doi.org/10.1007/s00442-008-1251-3

Jueterbock, A., Franssen, S. U., Bergmann, N., Gu, J., Coyer, J. A., Reusch, T. B. H., Bornberg-Bauer, E., & Olsen, J. L. (2016). Phylogeographic differentiation versus transcriptomic adaptation to warm temperatures in Zostera marina, a globally important seagrass. *Molecular Ecology*, *25*(21), 5396–5411. https://doi.org/10.1111/mec.13829

Kuzhiumparambil, U., Kumar, M., Nizio, K. D., Alonso, D., Gorst-Allman, P., Kelly, C., MacLeod, B., Forbes, S., & Ralph, P. (2022). Chapter 10 - Metabolomic profiling of anthropogenically threatened Australian seagrass Zostera muelleri using one- and two-dimensional gas chromatography☆. In D. J. Beale, K. E. Hillyer, A. C. Warden, & O. A. H. Jones (Eds.),

Applied Environmental Metabolomics (pp. 135–151). Academic Press. https://doi.org/https://doi.org/10.1016/B978-0-12-816460-0.00018-6

Lagerspetz, K. Y. H. (2006). What is thermal acclimation? *Journal of Thermal Biology*, *31*(4), 332–336. https://doi.org/https://doi.org/10.1016/j.jtherbio.2006.01.003

Larkum, A., Orth, R., & Duarte, C. (2006). *Seagrasses: Biology, Ecology and Conservation*. https://doi.org/10.1007/978-1-4020-2983-7_5

Lawson, C. A., Camp, E., Davy, S. K., Ferrier-Pagès, C., Matthews, J., & Suggett, D. J. (2022). Informing Coral Reef Conservation Through Metabolomic Approaches. In M. J. H. van Oppen & M. Aranda Lastra (Eds.), *Coral Reef Conservation and Restoration in the Omics Age* (pp. 179–202). Springer International Publishing. https://doi.org/10.1007/978-3-031-07055-6_12

Lenth R. (2023). *_emmeans: Estimated Marginal Means, aka Least-Squares Means_. R package version 1.8.4-1*. https://CRAN.R-project.org/package=emmeans

Liaw, A., & Wiener, M. (2002). Classification and Regression by randomForest. *R News*, *2*(3), 18–22.

Lüdecke D, Waggoner P, & Makowski D. (2019). Insight: A Unified Interface to Access Information from Model Objects in R . *Journal of Open Source Software*, *4*(38).

Marín-Guirao, L., Ruiz Fernandez, J., Dattolo, E., Garcia Muñoz, R., & Procaccini, G. (2016). Physiological and molecular evidence of differential short-Term heat tolerance in Mediterranean seagrasses. *Scientific Reports*, *6*, 28615. https://doi.org/10.1038/srep28615

Matyash, V., Liebisch, G., Kurzchalia, T. v, Shevchenko, A., & Schwudke, D. (2008). Lipid extraction by methyl-tert-butyl ether for high-throughput lipidomics*s. *Journal of Lipid Research*, *49*(5), 1137–1146. https://doi.org/https://doi.org/10.1194/jlr.D700041-JLR200

Meier, H. E. M., Dieterich, C., Gröger, M., Dutheil, C., Börgel, F., Safonova, K., Christensen, O. B., & Kjellström, E. (2022). Oceanographic regional climate projections for the Baltic Sea until 2100. In *Earth System Dynamics* (Vol. 13, Issue 1, pp. 159–199). Copernicus GmbH. https://doi.org/10.5194/esd-13-159-2022

Moksnes, P.-O., Emilia, M., Ohr, R. €, Holmer, M., Ekl € Of, J. S., Eriander, L., Infantes, E., Bostr, C., & Om, €. (2021). *COASTAL AND MARINE ECOLOGY Major impacts and societal costs of seagrass loss on sediment carbon and nitrogen stocks*. *12*(7). https://doi.org/10.1002/ecs2

Moreno-Mar In, F., Brun, F. G., & Pedersen, M. F. (2018). *Additive response to multiple environmental stressors in the seagrass Zostera marina L.* https://doi.org/10.1002/lno.10789

Nejrup, L. B., & Pedersen, M. F. (2008). Effects of salinity and water temperature on the ecological performance of Zostera marina. *Aquatic Botany*, *88*(3), 239–246. https://doi.org/10.1016/j.aquabot.2007.10.006

Nguyen, H. M., Kim, M., Ralph, P. J., Marín-Guirao, L., Pernice, M., & Procaccini, G. (2020). Stress Memory in Seagrasses: First Insight Into the Effects of Thermal Priming and the Role of Epigenetic Modifications. *Frontiers in Plant Science*, *11*. https://doi.org/10.3389/fpls.2020.00494

Oksanen J, Kindt R, & Simpson GL. (2023). *_vegan3d: Static and Dynamic 3D Plots for the "vegan" Package_*. *R package version 1.2-0*. https://CRAN.R-project.org/package=vegan3d

Oksanen J, Simpson G, Blanchet F, Kindt R, Legendre P, Minchin P, O'Hara R, Solymos P, Stevens M, Szoecs E, Wagner H, Barbour M, Bedward M, Bolker B, Borcard D, Carvalho G, Chirico M, De Caceres M, Durand S, … Furneaux B. (2022). *_vegan: Community Ecology Package_*. *R package version 2.6-4*. <https://CRAN.R-project.org/package=vegan>

Oliver, E. C. J., Donat, M. G., Burrows, M. T., Moore, P. J., Smale, D. A., Alexander, L. v, Benthuysen, J. A., Feng, M., sen Gupta, A., Hobday, A. J., Holbrook, N. J., Perkins-Kirkpatrick, S. E., Scannell, H. A., Straub, S. C., & Wernberg, T. (n.d.). Townsville MC, QLD 4810, Australia. 11 CSIRO Oceans and Atmosphere, Crawley, 6009 WA, Australia. 12 CSIRO Oceans and Atmosphere, Hobart, TAS 7000, Australia. 13 Australian Research Council Centre of Excellence for Climate Extremes. *Private Bag*, *3*(15). https://doi.org/10.1038/s41467-018-03732-9

Olsen, J. L., Rouzé, P., Verhelst, B., Lin, Y.-C., Bayer, T., Collen, J., Dattolo, E., De Paoli, E., Dittami, S., Maumus, F., Michel, G., Kersting, A., Lauritano, C., Lohaus, R., Töpel, M., Tonon, T., Vanneste, K., Amirebrahimi, M., Brakel, J., … Van de Peer, Y. (2016). The genome of the seagrass Zostera marina reveals angiosperm adaptation to the sea. *Nature*, *530*(7590), 331–335. https://doi.org/10.1038/nature16548

Olsen, Y. S., & Duarte, C. M. (2015). Combined effect of warming and infection by Labyrinthula sp. on the Mediterranean seagrass Cymodocea nodosa. *Marine Ecology Progress Series*, *532*, 101–109. https://www.int-res.com/abstracts/meps/v532/p101-109/

Patriquin, D. G. (1975). "Migration" of blowouts in seagrass beds at Barbados and Carriacou, West Indies, and its ecological and geological implications. *Aquatic Botany*, *1*, 163–189. https://doi.org/https://doi.org/10.1016/0304-3770(75)90021-2

Pazzaglia, J. (2022). *Living with global changes: physiological and molecular mechanisms as the basis for seagrasses resilience in a changing world*.

Pazzaglia, J., Badalamenti, F., Bernardeau-Esteller, J., Ruiz Fernandez, J., Giacalone, V., Procaccini, G., & Marín-Guirao, L. (2022). Thermo-priming increases heat-stress

tolerance in seedlings of the Mediterranean seagrass P. oceanica. *Marine Pollution Bulletin*, *174*, 113164. https://doi.org/10.1016/j.marpolbul.2021.113164

Pazzaglia, J., Nguyen, H. M., Santillán-Sarmiento, A., Ruocco, M., Dattolo, E., Marín-Guirao, L., & Procaccini, G. (2021a). *The Genetic Component of Seagrass Restoration: What We Know and the Way Forwards*. https://doi.org/10.3390/w13060829

Pazzaglia, J., Nguyen, H. M., Santillán-Sarmiento, A., Ruocco, M., Dattolo, E., Marín-Guirao, L., & Procaccini, G. (2021b). The Genetic Component of Seagrass Restoration: What We Know and the Way Forwards. *Water*, *13*(6). https://doi.org/10.3390/w13060829

Pazzaglia, J., Reusch, T. B. H., Terlizzi, A., Marín-Guirao, L., & Procaccini, G. (2021). Phenotypic plasticity under rapid global changes: The intrinsic force for future seagrasses survival. *Evolutionary Applications*, *14*(5), 1181–1201. https://doi.org/https://doi.org/10.1111/eva.13212

Pazzaglia, J., Santillán-Sarmiento, A., Helber, S. B., Ruocco, M., Terlizzi, A., Marín-Guirao, L., & Procaccini, G. (2020). Does Warming Enhance the Effects of Eutrophication in the Seagrass Posidonia oceanica? *Frontiers in Marine Science*, *7*. https://doi.org/10.3389/fmars.2020.564805

Plaisted, H. K., Shields, E. C., Novak, A. B., Peck, C. P., Schenck, F., Carr, J., Duffy, P. A., Evans, N. T., Fox, S. E., Heck, S. M., Hudson, R., Mattera, T., Moore, K. A., Neikirk, B., Parrish, D. B., Peterson, B. J., Short, F. T., & Tinoco, A. I. (2022). Influence of Rising Water Temperature on the Temperate Seagrass Species Eelgrass (Zostera marina L.) in the Northeast USA. *Frontiers in Marine Science*, *9*. https://doi.org/10.3389/fmars.2022.920699

R Core Team. (2022). R: A language and environment for statistical computing. . *R Foundation for Statistical Computing, Vienna, Austria*. https://www.R-project.org/

Reusch, T. B. H., Ehlers, A., Hä, A., & Worm, B. (2005). *Ecosystem recovery after climatic extremes enhanced by genotypic diversity*. www.pnas.orgcgidoi10.1073pnas.0500008102

Reusch, T. B. H., Schubert, P. R., Marten, S. M., Gill, D., Karez, R., Busch, K., & Hentschel, U. (2021). Lower Vibrio spp. abundances in Zostera marina leaf canopies suggest a novel ecosystem function for temperate seagrass beds. *Marine Biology*, *168*(10). https://doi.org/10.1007/S00227-021-03963-3

Röhr, M. E., Boström, C., Canal-Vergés, P., & Holmer, M. (2016). Blue carbon stocks in Baltic Sea eelgrass (Zostera marina) meadows. *Biogeosciences*, *13*(22), 6139–6153. https://doi.org/10.5194/bg-13-6139-2016

Salo, T., Reusch, T., & Boström, C. (2015). Genotype-specific responses to light stress in eelgrass Zostera marina, a marine foundation plant. *Marine Ecology Progress Series*, *519*. https://doi.org/10.3354/meps11083

Singh, B., & Sharma, R. A. (2015). Plant terpenes: defense responses, phylogenetic analysis, regulation and clinical applications. *3 Biotech*, *5*(2), 129–151. https://doi.org/10.1007/S13205-014-0220-2

Strobl C, Boulesteix A, Kneib T, Augustin T, & Zeileis A. (2008). Conditional Variable Importance for Random Forests. *BMC Bioinformatics*, *9*(307).

Sumner, L. W., Alexander, A. E., Ae, A., Ae, D. B., Ae, M. H. B., Beger, R., Daykin, C. A., Teresa, A. E., Fan, W.-M., Oliver, A. E., Ae, F., Goodacre, R., Julian, A. E., Griffin, L., Thomas, A. E., Ae, H., Hardy, N., James, A. E., Ae, H., … Goodacre, R. (2007). Proposed minimum reporting standards for chemical analysis Chemical Analysis Working Group (CAWG) Metabolomics Standards Initiative (MSI). *Metabolomics*, *3*, 211–221. https://doi.org/10.1007/s11306-007-0082-2

Trainor, P. J., DeFilippis, A. P., & Rai, S. N. (2017). Evaluation of Classifier Performance for Multiclass Phenotype Discrimination in Untargeted Metabolomics. *Metabolites*, *7*(2). https://doi.org/10.3390/metabo7020030

Unsworth, R. K. F., Collier, C. J., Waycott, M., Mckenzie, L. J., & Cullen-Unsworth, L. C. (2015). A framework for the resilience of seagrass ecosystems. *Marine Pollution Bulletin*, *100*(1), 34–46. https://doi.org/https://doi.org/10.1016/j.marpolbul.2015.08.016

Van de Peer, Y., Ma, X., Olsen, J. L., Reusch, T. B. H., Procaccini, G., Kudrna, D., Williams, M., Grimwood, J., Rajasekar, S., Jenkins, J., & Schmutz, J. (2021). Improved chromosome-level genome assembly and annotation of the seagrass, Zostera marina (eelgrass). *F1000Research*, *10*. https://doi.org/10.12688/f1000research.38156.1

Van Oppen, M. J. H., Oliver, J. K., Putnam, H. M., & Gates, R. D. (2015). Building coral reef resilience through assisted evolution. In *Proceedings of the National Academy of Sciences of the United States of America* (Vol. 112, Issue 8, pp. 2307–2313). National Academy of Sciences. https://doi.org/10.1073/pnas.1422301112

Ventura, D., Mancini, G., Casoli, E., Pace, D. S., Lasinio, G. J., Belluscio, A., & Ardizzone, G. (2022). Seagrass restoration monitoring and shallow-water benthic habitat mapping through a photogrammetry-based protocol. *Journal of Environmental Management*, *304*, 114262. https://doi.org/https://doi.org/10.1016/j.jenvman.2021.114262

von Nordheim, L., Kotterba, P., Moll, D., & Polte, P. (2018). Impact of Spawning Substrate Complexity on Egg Survival of Atlantic Herring (Clupea harengus, L.) in the Baltic Sea. *Estuaries and Coasts*, *41*(2), 549–559. https://doi.org/10.1007/s12237-017-0283-5

Wirries, J. (2023). *Effects of heat stress on the leaf histology of Zostera marina*.

Yu, L., Khachaturyan, M., Matschiner, M., Healey, A., Bauer, D., Cameron, B., Cusson, M., Emmet Duffy, J., Joel Fodrie, F., Gill, D., Grimwood, J., Hori, M., Hovel, K., Randall Hughes, A., Jahnke, M., Jenkins, J., Keymanesh, K., Kruschel, C., Mamidi, S., … H Reusch, T. B. (2022). *Ocean currents drive the worldwide colonization of the most*

widespread marine plant, eelgrass (Zostera marina). https://doi.org/10.1101/2022.12.10.519859

Appendix
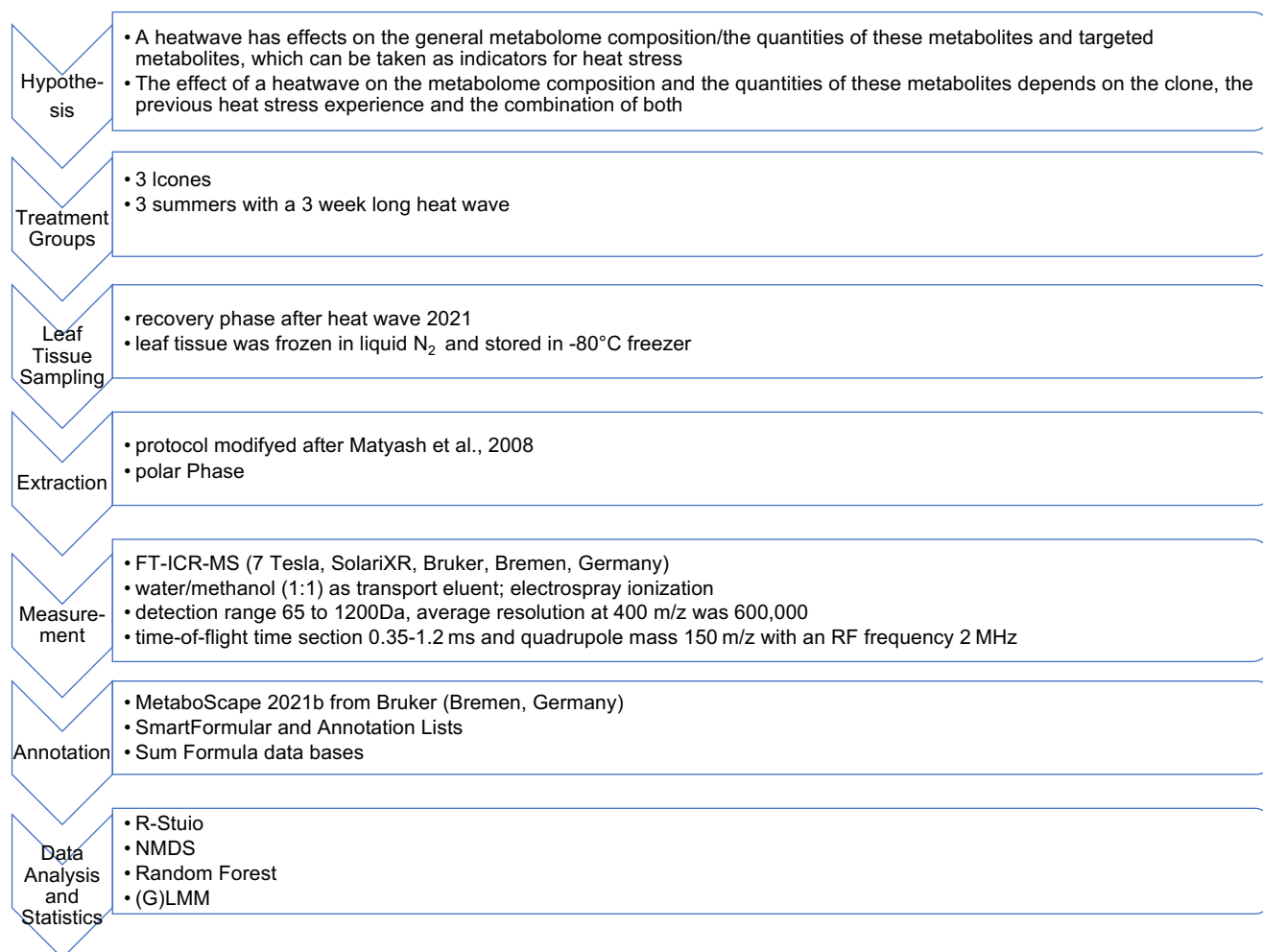
Figure 1: Overview of the workflow of the metabolomic assessment

Table 1: Growth rate means with standard errors

Mean ± SE	blue		red		yellow	
	cold	warm	cold	warm	cold	warm
Start heat wave	6.95±0.68	7.08±0.68	4.32±0.68	4.88±0.68	6.19±0.68	5.58±0.68
Mid heat wave	5.81±0.45	3.69±0.45	4.5±0.45	3.66±0.45	5.53±0.45	3.58±0.45
End heat wave	4.54±0.20	3.25±0.20	4.59±0.20	2.84±0.20	4.36±0.20	2.87±0.20
Recocery phase	5.14±0.41	3.94±0.41	3.35±0.41	3.16±0.41	4.34±0.41	3.93±0.41

Table 2: Molecular mass, sum formula and intensities of targeted metabolites measured via FT-ICR-MS

Metabolite	Molecular Mass	Sum Formula	Suggested Identity
M02	278,0324364	C8H22S5	
M03	305,9942329	C12H6N2O6S	
M06	144,042168	C6H8O4	Ethyl maleate
M13	215,0647647	C6H17NO3S2	
M14	191,0483705	C12H5N3	
M16	538,0351194	C14H26N4O8S5	
M18	246,0524385	C13H10O5	Phenylpropanoid
M19	284,0745371	C10H20O5S2	
M20	180,0634679	C6H12O6	Monosaccharide
M21	278,0404006	C10H10N6S2	
M23	216,040062	C5H13O7P	Monosaccharide
M25	264,0523818	C7H20O4S3	
M27	344,1231054	C23H20OS	
M28	240,9798314	C7H3N3O5S	
M29	228,0634507	C10H12O6	Monoterpenoid

Table 3: Intensities and metadata of targeted metabolites measured via FT-ICR-MS

Sample	Clone	Heat wave history	Heat wave 21	M02	M03	M06	M13	M14	M16	M18	M19	M20	M21	M23	M25	M27	M28	M29
1	blue	cold	warm	8,7104E+10	133904920	933896512	97180696	998319168	0	259486656	119017032	4,764E+10	5325683200	5,9354E+10	791899712	10604212	0	19979384
2	red	cold	warm	2,425E+10	38094008	134257232	169047600	69896392	0	68425408	15040970	1,4777E+10	735648064	1,7211E+10	251929600	15830737	0	12535168
3	yellow	cold	warm	3,0556E+10	37527208	191384432	94605288	128100808	0	58205896	21118640	1,1036E+10	691454656	1,1439E+10	258677760	0	0	10762601
4	blue	warm	warm	1,1871E+11	139824976	1315970944	0	0	104190720	395213920	108277456	0	3682858496	8,8487E+10	881802688	22295940	27039278	26081810
5	red	warm	warm	1,7883E+10	18378620	109131168	0	49076096	0	30466502	7296157	8193728512	183569200	1,1775E+10	91771568	37494948	32618464	0
6	yellow	warm	warm	3,2545E+10	45716292	245417584	283417184	136208528	14631622	78110000	29520904	1,8525E+10	1081601920	2,0951E+10	282443456	12783894	121402896	12830966
7	blue	cold	warm	5,7171E+10	86325224	588462400	153084144	527988640	56320212	146309056	66586996	2,9525E+10	2059473152	3,3992E+10	505285248	11554191	6602244	16051759
8	red	cold	warm	2,8025E+10	35553032	131656184	96077296	66256780	10399184	48259068	19686864	1,4048E+10	606703168	2,1543E+10	239074176	29133132	41688032	0
9	yellow	cold	warm	5,4616E+10	83159128	471995104	140040288	456308800	55261288	161896656	42623056	3,6643E+10	1285997056	4,0136E+10	502640416	18265872	83629144	10353406
10	blue	warm	cold	1,187E+11	148952608	1183823616	83602896	1755009792	124069656	320998912	121718912	5,6408E+10	7023101952	8,635E+10	885220416	0	29780512	47807544
11	red	warm	cold	2,2164E+10	32781924	174511504	219129248	58097540	10762810	58231816	16669756	1,4749E+10	560109824	1,9365E+10	196823680	31836684	50069864	0
12	yellow	warm	cold	3,1936E+10	44766168	337231968	136672016	123361128	23339730	111681312	26796398	2,1748E+10	807516992	2,2794E+10	268707200	17078274	120049680	9102243
13	blue	cold	cold	1,1971E+11	148256704	1110491904	97679456	2268697344	296911392	354468608	120207616	5,9821E+10	3656398848	1,1772E+11	812860544	31153910	44362128	39355791
14	red	cold	cold	0	31222168	165190656	255659728	58012616	10371610	58236564	13897626	1,2486E+10	506540672	1,8321E+10	196777136	32445292	49978036	0
15	yellow	cold	cold	3,3955E+10	47487064	304210528	120835616	173634384	0	83950888	30055286	1,8028E+10	1194138112	1,9988E+10	300598944	9274560	137966800	13566540
16	blue	warm	warm	7,3391E+10	0	816719488	114065856	0	0	214022144	96129072	3,7274E+10	2823060992	5,6358E+10	693593600	23343968	0	15737990
17	red	warm	warm	0	34983772	187081072	290043072	86245832	0	68090616	13406790	1,497E+10	0	2,4708E+10	199152992	44966948	0	0
18	yellow	warm	warm	3,9981E+10	67802776	391859712	152515296	218266320	0	126706568	38896796	2,3264E+10	1118246528	2,9548E+10	388779136	23307288	0	15004331
19	blue	warm	warm	5,7505E+10	86622032	636479040	135431280	380758432	35100980	169713936	53108452	3,1238E+10	1119007744	3,4782E+10	409020512	18866648	92426656	15789602
20	red	warm	warm	2,4907E+10	42251820	168685152	345156800	134735888	0	67647296	29730466	0	632650992	2,8992E+10	223025280	0	0	0
21	yellow	warm	warm	7,0224E+10	109577912	724391296	139330624	732778496	0	88099960	19450248	3,6069E+10	2362343424	2,133E+10	641878080	24705204	0	25952326
22	blue	cold	cold	9,9541E+10	0	1040184256	96292224	1453748480	160088256	257678544	125033392	4,4218E+10	5132433920	6,1736E+10	750161856	53115936	0	47395860
23	red	cold	cold	2,9728E+10	34098728	171958272	171233808	64894752	0	51877552	8741281	1,2596E+10	690681216	1,8839E+10	230578080	31480094	0	21584176
24	yellow	cold	cold	3,9627E+10	51963568	341858144	163611424	174027632	29653138	83763616	28436250	2,0645E+10	1212377600	2,6235E+10	280674688	19616542	11203912	23071052
25	blue	warm	warm	9,7463E+10	118569864	1034783872	74777016	0	113354368	231651952	112293768	3,6367E+10	3196291072	5,8893E+10	0	17482106	54287888	26796566
26	red	warm	warm	2,5907E+10	36687516	172657232	228029312	57933800	10365876	50398520	18692802	1,1324E+10	525260800	2,133E+10	211221264	44812320	36022792	18557940
27	yellow	warm	warm	5,3296E+10	79509744	518527488	161487680	467126176	88159616	125978688	39108096	2,7769E+10	1071329728	3,842E+10	421644576	20967592	111066896	13154879
28	blue	cold	cold	1,0119E+11	151162048	1104197376	106248472	1471382912	214173248	372356352	124610040	5,286E+10	6210253312	1,1703E+11	757911936	0	48048728	52140348
29	red	warm	cold	1,9652E+10	29205372	158570576	215647792	57179664	0	54293496	17409494	1,0743E+10	895692032	2,0276E+10	188772960	43564564	46006772	23729620
30	yellow	cold	warm	4,5469E+10	75835504	501419712	121463200	271181088	40848284	131885584	48922496	2,7531E+10	1808670848	3,5556E+10	340245184	23867934	130958184	25442996
31	blue	cold	cold	1,0721E+11	144660192	1190543104	91939512	1671414144	129715120	318439232	141184880	4,7446E+10	4369469952	1,374E+11	815704832	0	44816748	46312466
32	red	cold	cold	2,4989E+10	33354236	178981264	151830128	48910968	8887910	48695708	24067830	1,0795E+10	831351808	2,028E+10	211807856	38469348	48682724	20025978
33	yellow	cold	cold	6,3877E+10	51682452	510553920	116733672	136516720	14304099	109941848	63277320	1,7964E+10	1127868160	2,5892E+10	293783008	22738486	108247176	17448026
34	blue	warm	warm	8,2194E+10	124831608	1112411136	120789224	859034944	148411216	369031712	114601496	4,9002E+10	5584598016	1,0241E+11	648723072	0	38951360	53026486
35	red	warm	warm	2,6976E+10	20403934	132469824	168236544	30283942	0	31165872	9616324	5677099008	534662944	1,2252E+10	171616848	27380338	0	19106596
36	yellow	warm	cold	3,822E+10	55113744	347850592	132491128	194362768	26256602	94350064	43617628	1,8815E+10	1959700864	2,8151E+10	347616800	25474822	132028440	32262138

Declaration

I hereby declare that I have prepared this thesis independently and without outside assistance. I have not used any sources or aids other than those indicated. The submitted written version of the thesis corresponds to the one on the electronic storage medium. Furthermore, I certify that this work has not been submitted as a thesis elsewhere.

Kiel, 04.05.2023